(15) B. J. Hathaway and D. E. Billing, *Coord. Chem. Rev.*, **5**, 143 (1970).
(16) J. P. Collman, P. A. Christian, S. Current, P. Denisevich, T. R. Halbert, E. R. Schmitton, and K. O. Hodgson, *Inorg. Chem.*, **15**, 223 (1976).
(17) R. D. Shannon and C. T. Prewitt, *Acta Crystallogr., Sect. B*, **26**, 1076 (1970).
(18) J. Kohout, F. Valach, M. Quastlerova-Hvastijova, and J. Gazo, *Z. Phys. Chem. (Leipzig)*, **255**, 901 (1974).
(19) A. Pajumen and R. Hamalainen, *Suom. Kemistil. B*, **45**, 122 (1972).
(20) A. H. Norbury, *Adv. Inorg. Chem. Radiochem.*, **17**, 232 (1975).
(21) D. M. Duggan and D. N. Hendrickson, *Inorg. Chem.*, **13**, 2056 (1974).

Contribution from Ames Laboratory—DOE and the Department of Chemistry, Iowa State University, Ames, Iowa 50011

Synthesis and Characterization of New Metal–Metal Bonded Species. 2. Crystal and Molecular Structure of Dimeric Niobium(III) and Tantalum(III) Bromide Adducts with Tetrahydrothiophene. Direct Stereochemical Evidence of Bonding Electron Density in Confacial Bioctahedra with Metal–Metal Double Bonds

J. L. TEMPLETON, W. C. DORMAN, J. C. CLARDY, and R. E. McCARLEY*[1]

Received August 31, 1977

The previously reported niobium dimer $Nb_2Br_6(SC_4H_8)_3$ and the recently prepared tantalum analogue $Ta_2Br_6(SC_4H_8)_3$ have been characterized by complete structure determinations. Both compounds exist in the solid state as molecular confacial bioctahedrons with the two metal atoms of each dimer displaced from the center of their idealized octahedra toward one another. The Nb–Nb distance of 2.728 (5) Å and the Ta–Ta distance of 2.710 (2) Å are in accord with a formal metal–metal double bond. A distinctive feature of the structures is the unusually close approach of the two bromines in bridging positions of the confacial bioctahedra; this separation of only 3.30 Å is attributed to stereochemical activity of the two metal–metal π-bonding electrons. $Nb_2Br_6(SC_4H_8)_3$ crystallized in $P\bar{1}$ space group with $Z = 2$ and ρ(calcd) = 2.49 g cm^{-3} for a unit cell of dimensions $a = 15.088$ (8) Å, $b = 12.121$ (6) Å, $c = 8.981$ (2) Å, $\alpha = 112.93$ (3)°, $\beta = 77.32$ (2)°, and $\gamma = 125.23$ (2)°. Least-squares refinement of the structure resulted in a conventional agreement factor R_1 of 0.109 for 1870 reflections having $F^2 > 3\sigma(F^2)$. Crystals of $Ta_2Br_6(SC_4H_8)_3$ belonged to the $P\bar{1}$ space group with $Z = 2$ and ρ(calcd) = 2.98 g cm^{-3}. The cell dimensions were $a = 12.08$ (1) Å, $b = 12.74$ (1) Å, $c = 8.98$ (1) Å, $\alpha = 83.98$ (5)°, $\beta = 112.45$ (5)°, and $\gamma = 105.40$ (5)°. An R factor of 0.069 resulted from least-squares refinement of 1930 data points with $F > 3\sigma(F)$.

Introduction

The chemistry of the lower oxidation states of niobium and tantalum in discrete complexes remains relatively unexplored. The first structurally characterized halide complexes of niobium(III) were reported in 1970 as the metal–metal bonded binuclear salts $M_3Nb_2X_9$[2] (M = Rb, Cs; X = Cl, Br, I). Subsequently the molecular complexes $Nb_2X_6(SC_4H_8)_3$ (X = Cl, Br, I) were prepared and characterized by spectroscopic methods.[3] It was concluded that the molecules possessed the confacial bioctahedral structure with the S atom of one unique tetrahydrothiophene ligand occupying one of the three bridging positions. Magnetic data showed the compounds to be diamagnetic and a strong Nb–Nb interaction was inferred. In contrast, well-characterized tantalum(III) halide compounds are virtually unknown and therefore of considerable interest. A successful synthetic route to the tantalum dimers $Ta_2X_6(SC_4H_8)_3$ (X = Cl, Br) has been developed.[4] Physical methods of characterization showed that the tantalum compounds were entirely analogous to those of niobium. X-ray structural determinations of both $Nb_2Br_6(SC_4H_8)_3$ and $Ta_2Br_6(SC_4H_8)_3$ were undertaken in order to clearly delineate any differences between them. In related complexes of molybdenum(III) and tungsten(III) containing the anions $M_2X_9^{3-}$ the W–W distance is much shorter, 2.41 Å in $K_3W_2Cl_9$,[5] than the Mo–Mo distance in $Cs_3Mo_2Cl_9$,[6] 2.66 Å. Therefore it was of great interest to see if the Ta–Ta and Nb–Nb bond lengths would differ so markedly.

Experimental Section

The two compounds were prepared according to methods described elsewhere.[3,4] Crystals suitable for x-ray data collection were obtained by recrystallization of the materials from toluene solutions which had been saturated at room temperature, filtered, and cooled slowly to ca. −15 °C to induce crystal growth. The very air-sensitive crystals were then sealed in Lindemann glass capillaries under nitrogen.

Data Collection and Reduction. Crystals of both $Nb_2Br_6(SC_4H_8)_3$ and $Ta_2Br_6(SC_4H_8)_3$ were examined by precession and Weissenberg film techniques and both exhibited $\bar{1}$ Laue symmetry indicating a triclinic space group. No systematic absences were observed. Lattice parameters were determined for the niobium compound by least-squares fit to 12 independent reflection angles whose centers were determined by left–right, top–bottom beam splitting on a previously aligned Hilger-Watts four-circle diffractometer (Cu Kα radiation, λ 1.5418 Å). Any error in the instrumental zero was eliminated by centering the reflection at both $+2\theta$ and -2θ. For the tantalum compound a similar procedure was used, but only three independent reflection angles and Mo Kα radiation (λ 0.71069 Å) were employed. The following lattice parameters were found: for $Nb_2Br_6(SC_4H_8)_3$ $a = 15.088$ (8) Å, $b = 12.121$ (6) Å, $c = 8.981$ (2) Å, $\alpha = 112.93$ (3)°, $\beta = 77.32$ (2)°, and $\gamma = 125.23$ (2)° with $Z = 2$ and ρ(calcd) = 2.49 g cm^{-3}; for $Ta_2Br_6(SC_4H_8)_3$ $a = 12.08$ (1) Å, $b = 12.74$ (1) Å, $c = 8.98$ (1) Å, $\alpha = 83.98$ (5)°, $\beta = 112.45$ (5)°, and $\gamma = 105.40$ (5)° with $Z = 2$ and ρ(calcd) = 2.98 g cm^{-3}.

The crystals chosen for data collection had approximate dimensions as follows along the a, b, and c axes, respectively: for $Nb_2Br_6(SC_4H_8)_3$ 0.270, 0.050, and 0.045 mm and for $Ta_2Br_6(SC_4H_8)_3$ 0.06, 0.08, and 0.40 mm. Integrated intensities were measured using Ni-filtered Cu Kα and Zr-filtered Mo Kα radiation, respectively, for the niobium and tantalum compounds, using the θ–2θ scanning technique on the automated diffractomer cited earlier. A counting rate of 0.2048 s per step of 0.01° in θ was employed with a variable scan range of 50 steps plus two steps per degree θ. Stationary crystal, stationary counter background measurements were made at the beginning and end of each scan for half the total scan time. All data were collected within a 2θ sphere of 55° for the niobium and 45° for the tantalum compounds, respectively, in each of four octants; a total of 3500 and 3216 reflections were monitored in the respective cases.

As a general check on electronic and crystal stability the intensities of three standard reflections were measured every 50 reflections during the data collection period. For the niobium compound the total decrease in intensity of these reflections was only 15% and the data were appropriately corrected. However, for the tantalum compound the intensities of the standard reflections decreased to only 20% of the original intensities by termination of data collection. A linear least-squares fit of standard intensities vs. the number of data points monitored (n) was made using a weighting factor of $1/C_t$ for the intensities (C_t = total counts). The correlation coefficient was >0.99

0020-1669/78/1317-1263$01.00/0

Table I. Positional and Thermal Parameters ($\times 10^4$) and Their Estimated Standard Deviations[a] for $Nb_2Br_6(SC_4H_8)_3$

Atom	x	y	z	β_{11}	β_{22}	β_{33}	β_{12}	β_{13}	β_{23}
Nb(1)	0.2891 (3)	0.1484 (4)	0.2142 (5)	42 (3)	81 (5)	104 (7)	26 (4)	−55 (4)	39 (5)
Nb(2)	0.2118 (3)	−0.0997 (4)	0.2667 (4)	32 (3)	68 (5)	96 (8)	23 (3)	−11 (4)	20 (4)
Br(1)	0.4368 (5)	0.2310 (6)	0.0103 (7)	83 (6)	215 (11)	227 (13)	88 (7)	47 (7)	130 (10)
Br(2)	0.3500 (5)	0.3786 (5)	0.4496 (6)	70 (5)	75 (7)	220 (12)	14 (5)	−51 (7)	4 (7)
Br(3)	0.2817 (5)	−0.2608 (5)	0.1074 (7)	76 (5)	129 (8)	207 (11)	68 (5)	7 (6)	42 (8)
Br(4)	0.2052 (5)	−0.1088 (5)	0.5464 (6)	93 (6)	102 (8)	153 (11)	42 (5)	−40 (6)	41 (7)
Br(5)	−0.1762 (5)	0.1019 (5)	0.0106 (6)	81 (6)	116 (8)	115 (10)	52 (5)	−13 (6)	26 (7)
Br(6)	0.1051 (5)	0.0256 (6)	0.3593 (7)	67 (5)	181 (10)	232 (13)	62 (6)	−24 (7)	40 (9)
S(1)	0.401 (1)	0.103 (1)	0.323 (1)	36 (10)	113 (17)	135 (23)	39 (11)	39 (13)	58 (16)
S(2)	0.193 (1)	0.237 (1)	0.130 (1)	110 (15)	115 (18)	155 (26)	87 (14)	17 (16)	26 (17)
S(3)	0.012 (1)	−0.337 (1)	0.217 (1)	51 (11)	60 (15)	191 (26)	11 (10)	−46 (14)	24 (16)

Atom	x	y	z	B_{iso}, Å^2	Atom	x	y	z	B_{iso}, Å^2
C(1)	0.516 (4)	0.097 (4)	0.217 (5)	3.4 (10)	C(7)	0.187 (5)	0.244 (6)	−0.155 (6)	7.1 (15)
C(2)	0.607 (5)	0.208 (5)	0.348 (6)	6.3 (10)	C(8)	0.128 (4)	0.134 (5)	−0.084 (5)	5.2 (12)
C(3)	0.562 (5)	0.211 (5)	0.507 (6)	6.0 (10)	C(9)	0.024 (3)	−0.479 (4)	0.241 (5)	3.1 (10)
C(4)	0.464 (3)	0.218 (3)	0.527 (4)	1.5 (8)	C(10)	0.087 (4)	0.548 (5)	−0.337 (6)	5.5 (13)
C(5)	0.314 (4)	0.414 (5)	0.105 (6)	5.0 (12)	C(11)	0.097 (4)	0.442 (5)	−0.445 (6)	5.1 (13)
C(6)	0.292 (6)	0.394 (7)	−0.076 (8)	10.3 (20)	C(12)	0.070 (4)	0.310 (5)	−0.340 (5)	4.7 (12)

[a] The form of the anisotropic thermal parameter is $\exp[-(\beta_{11}h^2 + \beta_{22}k^2 + \beta_{33}l^2 + \beta_{12}hk + \beta_{13}hl + \beta_{23}kl)]$. Here and in other tables, numbers in parentheses are the estimated standard deviations in the least significant digits.

Table II. Positional and Thermal Parameters ($\times 10^4$) and Their Estimated Standard Deviations for $Ta_2Br_6(SC_4H_8)_3$

Atom	x	y	z	β_{11}	β_{22}	β_{33}	β_{12}	β_{13}	β_{23}
Ta(1)	−0.3118 (1)	0.2873 (1)	0.2651 (2)	81 (1)	47 (1)	116 (3)	7 (1)	44 (2)	−12 (2)
Ta(2)	−0.1428 (1)	0.2090 (1)	0.2111 (2)	83 (2)	48 (2)	135 (3)	7 (1)	48 (2)	−17 (2)
Br(1)	−0.3144 (4)	0.2954 (3)	0.5429 (5)	142 (5)	80 (3)	120 (8)	37 (3)	74 (5)	0 (4)
Br(2)	−0.5401 (3)	0.2196 (3)	0.1092 (6)	76 (4)	73 (3)	230 (10)	0 (3)	45 (5)	41 (5)
Br(3)	0.0271 (4)	0.1494 (3)	0.4425 (5)	109 (4)	65 (3)	183 (9)	29 (3)	52 (5)	16 (5)
Br(4)	−0.2066 (4)	0.0622 (3)	0.0082 (6)	138 (5)	73 (3)	236 (10)	−2 (3)	95 (6)	−69 (5)
Br(5)	−0.0807 (3)	0.3958 (3)	0.3578 (5)	80 (4)	50 (3)	145 (8)	4 (3)	40 (4)	26 (4)
Br(6)	−0.2767 (4)	0.3255 (3)	−0.0111 (5)	108 (4)	80 (3)	116 (8)	24 (3)	53 (5)	0 (4)
S(1)	−0.2897 (9)	0.1044 (8)	0.3215 (13)	117 (11)	52 (7)	187 (22)	5 (7)	66 (13)	−30 (11)
S(2)	−0.3515 (9)	0.4828 (7)	0.2177 (14)	130 (11)	43 (7)	207 (24)	22 (7)	95 (14)	2 (11)
S(3)	0.0430 (9)	0.3060 (8)	0.1216 (13)	95 (10)	86 (9)	175 (22)	10 (8)	66 (13)	−19 (12)

Atom	x	y	z	B_{iso}, Å^2	Atom	x	y	z	B_{iso}, Å^2
C(1)	−0.245 (3)	0.043 (3)	0.528 (5)	4.3 (8)	C(7)	−0.460 (4)	0.596 (3)	0.329 (5)	5.4 (9)
C(2)	−0.361 (5)	−0.062 (5)	0.497 (8)	10.2 (16)	C(8)	−0.497 (3)	0.483 (3)	0.240 (5)	4.7 (8)
C(3)	−0.394 (5)	−0.104 (5)	0.348 (8)	9.5 (15)	C(9)	0.116 (4)	0.202 (3)	0.097 (5)	5.6 (9)
C(4)	−0.421 (3)	−0.015 (3)	0.213 (5)	5.1 (9)	C(10)	0.102 (5)	0.222 (5)	−0.077 (8)	8.9 (14)
C(5)	−0.243 (4)	0.574 (3)	0.396 (6)	5.9 (10)	C(11)	0.038 (7)	0.288 (7)	−0.170 (10)	14.1 (23)
C(6)	−0.336 (4)	0.606 (3)	0.450 (5)	5.5 (9)	C(12)	−0.016 (5)	0.349 (4)	−0.088 (7)	8.4 (13)

for each of the three standards, thus indicating the validity of the fit. The average slope of I_n/I_0 (I_n = intensity of standard after n data points collected) vs. n was -2.47×10^{-4}. Thus the data were quite accurately corrected for crystal decay by $I_0 = I_n(1-2.47 \times 10^{-4}n)^{-1}$ prior to further data reduction. The error introduced by this correction procedure can be incorporated into the expression for $[\sigma(I)]^2$ as follows:

$$[\sigma(I)]^2 = K_n^2 C_t + K_n^2 C_b + (C_t - C_b)^2 \sigma_{K_n}^2 + (0.3K_n C_t)^2 + (0.3K_n C_b)^2$$

where K_n is the scale factor $(1-2.47 \times 10^{-4}n)^{-1}$, σ_{K_n} is the absolute error associated with K_n, and C_b is the background count.

Intensities were then corrected for Lorentz–polarization effects. Because of the relatively large crystal and large absorption coefficient (μ = 229.38 cm^{-1}) the data for the niobium compound were corrected for absorption using the TALABS program.[7] Maximum and minimum transmission factors were 0.4187 and 0.0783, respectively, for the crystal of the niobium compound. In view of the very large corrections necessitated by crystal decay it was deemed inadvisable to also apply an absorption correction to the data for the tantalum compound. A total of 1870 and 1930 data points having $F^2 \geq 3\sigma(F^2)$ and $F > 3\sigma(F)$, respectively, for the niobium and tantalum compounds were used in the subsequent structure refinements.

Solution and Refinement of the Structures. In both cases the metal atom positions were readily located from sharpened Patterson functions, as were also the Br atoms in the niobium compound. Succeeding structure factor and electron density calculations based on the heavy-atom phasing located the remaining Br, S, and C atom positions. These positions were refined by full-matrix least-squares techniques,[8] including anisotropic motion on all except the carbon atom positions. The scattering factors used were those of Hanson et al.,[9] with Nb, Ta, Br, and S modified for the real and imaginary parts of anomalous dispersion.[10] For the niobium compound refinement converged to $R_1 = \sum||F_o| - |F_c||/\sum|F_o| = 0.109$ and $R_2 = [\sum w(||F_o| - |F_c||)^2/\sum w|F_o|^2]^{1/2} = 0.113$. For the tantalum compound the final values were $R_1 = 0.069$ and $R_2 = 0.070$. There were no peaks of greater than 1 e/Å^3 on the final electron density difference maps. Final positional and thermal parameters for the nonhydrogen atoms, along with their standard deviations as estimated from the inverse matrix,[11] are included in Tables I and II. A listing of observed and calculated structure factors is available.[12]

Results and Discussion

Description of the Structures. The molecular structure of both $Nb_2Br_6(SC_4H_8)_3$ and $Ta_2Br_6(SC_4H_8)_3$ is that of a confacial bioctahedron as shown in Figure 1, including the same orientation of the tetrahydrothiophene rings with respect to the remainder of the molecule. There are few significant differences in the structural parameters of the two molecules as reflected in the bond distances and angles listed in Tables III and IV. Some important nonbonded distances in $Ta_2Br_6(SC_4H_8)_3$ are given in Table V.

The shared trigonal face consists of one tetrahydrothiophene ligand and two bromides with the pseudooctahedral environment around each metal atom completed by two terminal bromides and one terminal sulfur ligand. The bridging tetrahydrothiophene ligand is trans to both terminal sulfur ligands

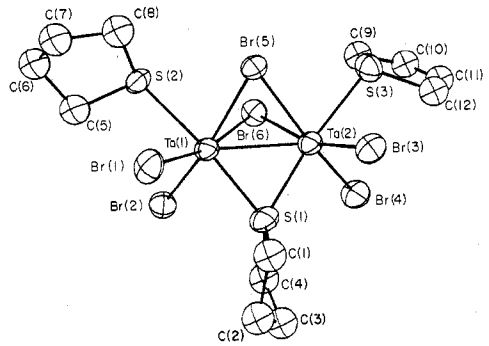

Figure 1. An ORTEP view of the $Ta_2Br_6(SC_4H_8)_3$ molecule showing 50% probability ellipsoids and atomic numbering scheme. The numbering scheme is also the same for $Nb_2Br_6(SC_4H_8)_3$.

Table III. Bond Distances (A)[a]

Bond	$Nb_2Br_6(SC_4H_8)_3$	$Ta_2Br_6(SC_4H_8)_3$
M(1)-M(2)	2.728 (5)	2.710 (2)
M(1)-Br(5)	2.638 (6)	2.611 (3)
M(1)-Br(6)	2.604 (7)	2.647 (4)
M(2)-Br(5)	2.648 (6)	2.630 (3)
M(2)-Br(6)	2.615 (8)	2.643 (5)
Av M-Br (b)[b]	2.626	2.633
M(1)-Br(1)	2.526 (7)	2.519 (4)
M(1)-Br(2)	2.529 (6)	2.519 (4)
M(2)-Br(3)	2.552 (7)	2.519 (5)
M(2)-Br(4)	2.530 (6)	2.507 (3)
Av M-Br (t)[b]	2.534	2.516
M(1)-S(1)	2.519 (14)	2.396 (10)
M(2)-S(1)	2.455 (12)	2.390 (10)
Av M-S (b)	2.487	2.393
M(1)-S(2)	2.591 (16)	2.620 (9)
M(2)-S(3)	2.673 (12)	2.627 (10)
Av M-S (t)	2.632	2.624
S(1)-C(1)	1.81 (5)	1.869 (43)
S(1)-C(4)	1.86 (4)	1.901 (35)
S(2)-C(5)	1.92 (5)	1.900 (39)
S(2)-C(8)	1.94 (5)	1.840 (37)
S(3)-C(9)	1.92 (5)	1.849 (41)
S(3)-C(12)	1.87 (5)	1.825 (59)
C(1)-C(2)	1.56 (6)	1.61 (6)
C(2)-C(3)	1.43 (6)	1.37 (7)
C(3)-C(4)	1.49 (6)	1.57 (7)
C(5)-C(6)	1.62 (7)	1.53 (5)
C(6)-C(7)	1.58 (7)	1.45 (5)
C(7)-C(8)	1.42 (6)	1.60 (5)
C(9)-C(10)	1.60 (6)	1.50 (7)
C(10)-C(11)	1.34 (6)	1.31 (9)
C(11)-C(12)	1.60 (6)	1.52 (8)

[a] Atoms are labeled as in Figure 1. [b] Key: b, bridge; t, terminal.

such that an effective symmetry of C_{2v} pertains to the molecule if only the metal, Br, and S atoms are considered. No symmetry restrictions are crystallographically imposed on the structures.

Strong metal–metal bonding is reflected in the M–M distances: Nb–Nb, 2.728 (5) Å; Ta–Ta, 2.710 (2) Å. A further indication of strong metal–metal attraction is the displacement of the metal atoms toward one another and away from the center of their respective idealized octahedra by ca. 0.20 Å in each case. Since the compounds are diamagnetic, it may be concluded that the two d electrons of each metal atom are paired, and indeed a metal–metal bond, formally of bond order 2, must exist in these molecules. The effect of the number of electrons formally entering into metal–metal bonding in confacial bioctahedral structures can be seen roughly by comparing the metal–metal distances found here with the distances and formal bond order (n) for the following

Table IV. Bond Angles (deg)

	$Nb_2Br_6(SC_4H_8)_3$	$Ta_2Br_6(SC_4H_8)_3$
M-Bridge-M Angles		
M(1)-Br(5)-M(2)	62.1 (2)	62.3 (1)
M(1)-Br(6)-M(2)	63.0 (2)	61.6 (1)
M(1)-S(1)-M(2)	66.5 (3)	69.0 (3)
Bridge-M-Bridge Angles		
Br(5)-M(1)-Br(6)	78.2 (2)	77.7 (1)
Br(5)-M(2)-Br(6)	77.8 (2)	77.4 (1)
Br(5)-M(1)-S(1)	100.0 (3)	100.8 (3)
Br(5)-M(2)-S(1)	101.5 (3)	100.4 (2)
Br(6)-M(1)-S(1)	101.4 (3)	101.3 (3)
Br(6)-M(2)-S(1)	102.8 (3)	101.5 (3)
Br-M-Br Angles		
Br(1)-M(1)-Br(2)	101.9 (2)	99.6 (2)
Br(3)-M(2)-Br(4)	99.7 (2)	102.0 (2)
Br(1)-M(1)-Br(5)	89.4 (2)	91.9 (1)
Br(2)-M(1)-Br(6)	89.2 (2)	89.1 (1)
Br(3)-M(2)-Br(5)	88.8 (2)	89.0 (1)
Br(4)-M(2)-Br(6)	92.3 (2)	90.0 (2)
S-M-Br Angles		
S(1)-M(1)-Br(1)	88.4 (3)	88.7 (3)
S(1)-M(1)-Br(2)	89.8 (3)	91.0 (3)
S(2)-M(1)-Br(5)	88.9 (3)	82.9 (2)
S(2)-M(1)-Br(6)	81.6 (4)	83.5 (3)
S(2)-M(1)-Br(1)	90.5 (3)	87.0 (3)
S(2)-M(1)-Br(2)	81.8 (3)	86.1 (2)
S(1)-M(2)-Br(3)	88.2 (3)	89.4 (3)
S(1)-M(2)-Br(4)	87.9 (3)	89.8 (2)
S(3)-M(2)-Br(5)	83.7 (3)	81.9 (2)
S(3)-M(2)-Br(6)	82.7 (3)	87.6 (3)
S(3)-M(2)-Br(3)	87.2 (3)	81.7 (3)
S(3)-M(2)-Br(4)	87.7 (3)	89.7 (2)
Trans Angles		
S(1)-M(1)-S(2)	171.0 (4)	174.4 (3)
S(1)-M(2)-S(3)	173.0 (5)	170.8 (4)
Br(5)-M(1)-Br(2)	165.3 (3)	163.7 (2)
Br(5)-M(2)-Br(4)	167.7 (3)	165.1 (2)
Br(6)-M(1)-Br(1)	165.3 (3)	166.6 (1)
Br(6)-M(2)-Br(3)	164.0 (2)	163.9 (1)

Table V. Nonbonded Distances in $Ta_2Br_6(SC_4H_8)_3$ (A)

Br(1)-Br(2)	3.848 (6)	S(1)-Br(5)	3.862 (9)
Br(3)-Br(4)	3.904 (6)	S(1)-Br(6)	3.902 (13)
Av Br_t-Br_t[a]	3.876	Av S_b-Br_b	3.882
Br(1)-Br(5)	3.686 (5)	S(2)-Br(1)	3.539 (12)
Br(3)-Br(5)	3.611 (6)	S(2)-Br(2)	3.509 (9)
Br(2)-Br(6)	3.626 (6)	S(3)-Br(3)	3.366 (13)
Br(4)-Br(6)	3.643 (6)	S(3)-Br(4)	3.622 (10)
Av Br_t-Br_b	3.642	Av S_t-Br_t	3.509
$Br(5)_b$-$Br(6)_b$	3.298 (5)	S(2)-Br(5)	3.464 (11)
S(1)-Br(1)	3.438 (9)	S(2)-Br(6)	3.506 (9)
S(1)-Br(2)	3.507 (12)	S(3)-Br(5)	3.445 (10)
S(1)-Br(3)	3.455 (11)	S(3)-Br(6)	3.649 (11)
S(1)-Br(4)	3.458 (11)	Av S_t-Br_b	3.516
Av S_b-Br_t	3.465		

[a] Key: b, bridging; t, terminal.

anions: $W_2Cl_9^{3-}$, 2.41 Å,[5] n = 3.0; $W_2Br_9^{2-}$, 2.601 Å,[15] n = 2.5; $Nb_2Cl_9^{3-}$, 2.70 Å,[2] n = 2.0. Because of the delicate interplay of attractive and repulsive forces within confacial bioctahedral structures such comparisons should be regarded with caution.[13]

The metal–bromine bond lengths show the expected differences as illustrated by the average Nb–Br_b and Ta–Br_b distances which are 0.09 and 0.12 Å longer, respectively, than the average M–Br_t distances. For species with the confacial bioctahedral structure the bridging metal–halide bonds are typically longer than the corresponding terminal bonds.[13] Results of a study of the ^{81}Br NQR frequencies in these compounds are consistent with the bridging bromine atoms

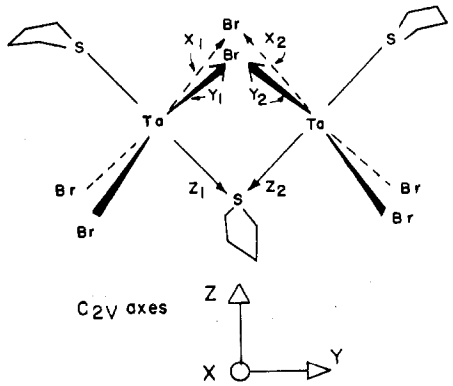

Figure 2. Diagram showing choice of local symmetry coordinates of metal atoms in the confacial bioctahedral dimers.

entering into only σ bonding with the metal atoms but with the terminal bromine atoms participating in both σ and π bonding.[4] The shorter M–Br_t distances of course correlate well with the enhanced π bonding.

In contrast to the M–Br bonding the inverse relationship is observed for M–S_b vs. M–S_t distances. The M–S_b bonds are markedly shorter than the M–S_t bonds, by an average of 0.14 and 0.23 Å, respectively, for the niobium and tantalum cases. Although the average M–S_t distances are almost the same in the two molecules (2.63 (1) and 2.62 (1) Å), the average M–S_b distances differ significantly, viz., 2.48 (1) and 2.39 (1) Å for Nb–S_b and Ta–S_b, respectively. An explanation for this difference is not readily apparent.

Steric considerations can account for the large discrepancy between the M–S_t and M–S_b distances as follows. The four Br atoms bound to each metal form a least-squares plane to within 0.01 Å, but the metal–metal attraction pulls the metal atoms out of these planes, e.g., by 0.222 and 0.211 Å for Ta(1) and Ta(2), respectively. The terminal S atoms are hindered from closer approach to the metal atoms by repulsion of the four cis Br atoms in the plane, e.g., as evidenced by the relatively short nonbonded S_t–Br distance of 3.51 Å in the tantalum compound. On the other hand the S atom of the bridging ligand is not sterically hindered; i.e., the two metal atoms have moved toward it and consequently the M–S_b distance is much shorter. In fact, in the tantalum compound the Ta–S_b distance of 2.39 Å is less than the sum of covalent radii for S (1.04 Å) and Ta (1.38 Å), where the latter value is derived from the covalent radius of Br (1.14 Å) and the average Ta–Br_t distance of 2.516 Å.

Discussion of Electronic Effects. The nonbonded distances within both molecules are in general agreement with accepted van der Waals limits with one outstanding exception; viz., the two Br atoms in bridging positions are within 3.30 Å of each other. The tantalum dimer will be used to illustrate the details of this distortion, but the argument applies equally well to the niobium dimer. Repulsion between the bridging S atom and the bridging Br atoms can be quickly discounted as the cause of this close Br–Br contact since the average S_b–Br_b distance of 3.88 Å is longer than any of the other nonbonded contacts in the molecule (Table V). To satisfactorily explain this anomaly, electronic effects as derived from the MO description of the dimer must be examined.

It will be useful to invoke a descent from the D_{3h} symmetry of an $M_2X_9^{n-}$ confacial bioctahedral dimer (with metal–metal bonding) to the effective C_{2v} symmetry of $Ta_2Br_6(SC_4H_8)_3$. The most lucid axes of quantization for the two metal atoms will be employed as defined in Figure 2, but of course equivalent results are obtained when the metal–metal axis is chosen as the z axis for both metal atoms. With this choice of axes the orbitals of interest will be those not involved in metal ligand σ bonding, viz., the d_{xz}, d_{yz}, and d_{xy} orbitals on

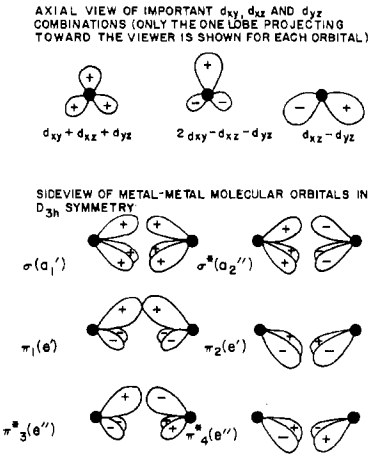

Figure 3. Metal–metal molecular orbital overlap diagram for a confacial bioctahedron of D_{3h} symmetry.

each metal atom. Neglecting any π interactions with the ligands the symmetry adapted linear combinations in D_{3h} symmetry are given in eq 1–6. Based on overlap consider-

$$\sigma(a_1') = 6^{-1/2}[d_{xy}(1) + d_{xz}(1) + d_{yz}(1) + d_{xy}(2) + d_{xz}(2) + d_{yz}(2)] \quad (1)$$

$$\sigma^*(a_2'') = 6^{-1/2}[d_{xy}(1) + d_{xz}(1) + d_{yz}(1) - d_{xy}(2) - d_{xz}(2) - d_{yz}(2)] \quad (2)$$

$$\pi_1(e') = 12^{-1/2}[2d_{xy}(1) - d_{xz}(1) - d_{yz}(1) + 2d_{xy}(2) - d_{xz}(2) - d_{yz}(2)] \quad (3)$$

$$\pi_2(e') = 4^{-1/2}[d_{xz}(1) - d_{yz}(1) + d_{xz}(2) - d_{yz}(2)] \quad (4)$$

$$\pi_3^*(e'') = 12^{-1/2}[2d_{xy}(1) - d_{xz}(1) - d_{yz}(1) - 2d_{xy}(2) + d_{xz}(2) + d_{yz}(2)] \quad (5)$$

$$\pi_4^*(e'') = 4^{1/2}[d_{xz}(1) - d_{yz}(1) - d_{xz}(2) + d_{yz}(2)] \quad (6)$$

ations shown in Figure 3 these MO's will result in the energy level scheme $a_1' < e' < e'' < a_2''$, where the $\sigma(a_1')$ and $\pi(e')$ orbitals are bonding and the $\pi(e'')$ and $\sigma(a_2'')$ orbitals are antibonding. Metal–metal orbitals and an energy level ordering in agreement with this have been previously proposed.[14]

For an appropriate MO description of the metal–metal bonding in $Ta_2Br_6(SC_4H_8)_3$ the descent in symmetry to C_{2v} is necessary. The diamagnetic behavior of the $M_2X_6(SC_4H_8)_3$ dimers must be a consequence of splitting the $\pi(e')$ energy levels substantially in the lower C_{2v} symmetry so that spin pairing occurs. In the absence of such splitting the ground state would be $[\sigma(a_1')]^2[\pi(e')]^2$, $^3A_2'$, as evidently is the case for the salts $M_3Nb_2X_9$ (M = Rb, Cs; X = Br, I).[2] The crux of the procedure is to establish which π orbital is lowered in energy, and therefore occupied, and which is unoccupied. It is here that the unusually close contact between the bridging Br atoms and large S_b–Br_b distances provide important evidence.

The linear combinations listed in eq 1–6 and illustrated in Figure 3 for D_{3h} symmetry are still valid MO's, but the descent in symmetry converts them to the following representations in the C_{2v} group: $a_1'(\sigma) \rightarrow a_1$, $a_2''(\sigma^*) \rightarrow b_2$, $e'(\pi_1) \rightarrow a_1$, $e'(\pi_2) \rightarrow b_1$, $e''(\pi_3^*) \rightarrow b_2$, and $e''(\pi_4^*) \rightarrow a_2$. The a_1 MO derived from a_1' remains as σ bonding and should have the lowest energy of the set; two electrons are therefore assigned to this orbital. An inspection of the a_1 π orbital (derived from e′) reveals that the region of greatest overlap lies between the two bridging Br atoms with minor overlap present in the spaces between the bridging S and bridging Br atoms. A similar examination of the b_1 π orbital (derived from e′) shows no contribution from the two d_{xy} orbitals between the bridging atoms, but rather the entire π bond results from overlap of d_{xz} and d_{yz} orbitals of the two metal atoms in the spaces

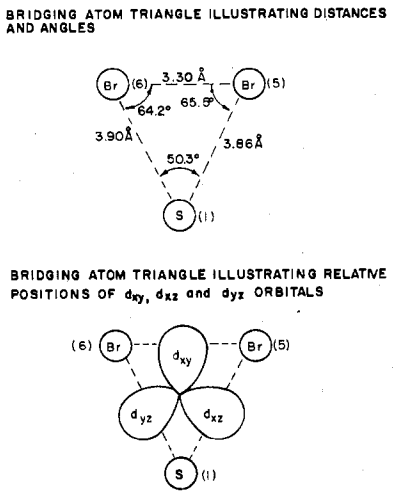

Figure 4. View along the metal–metal axis of the triangle formed by the bridging ligands of $M_2Br_6(SC_4H_8)_3$ dimers.

between the S and two Br atoms. Thus the b_1 π orbital is assessed as the lower in energy and occupied with the remaining electron pair.

A view along the metal–metal axis of the triangle formed by the three bridging atoms as shown in Figure 4 emphasizes the role of the lower energy π orbital. Even though the van der Waals radius of sulfur is less than that of bromine, the S–Br distances are 0.60 and 0.56 Å longer than the Br–Br separation of 3.30 Å. In conjunction with the large S_b–Ta–Br_b angles which average 101.0° compared to the Br_b–Ta–Br_b average angle of 77.6° it seems that the b_1 π orbital effectively fills the voids between the S and Br atoms with electron density which repels the bridging ligands. Thus the observed distortion of the structure in the bridging region of the molecule bears direct witness to the stereochemical activity of π electrons in the metal–metal bond. The unique opportunity to observe this effect is afforded by these molecules because of the lower symmetry induced by the bridging tetrahydrothiophene ligand and the total of only four electrons entering into metal–metal bonding so that one of the π orbitals remains empty and an unbalanced π-bonding electron density distribution results. Because of the observed distortion the stability of the b_1 π orbital is enhanced and the a_1 π orbital, though empty, is destabilized.

Conclusion

The structures found here confirm the 3+ oxidation state of both niobium and tantalum. Although Nb(III) has been previously reported in the $Nb_2X_9^{3-}$ salts,[2] the confirmation of Ta(III) in this halide dimer is particularly noteworthy. An interesting contrast is provided by the diamagnetic $M_2X_6(SC_4H_8)_3$ molecules[3,4] on one hand and the paramagnetic salts of $Nb_2X_9^{3-}$ on the other, even though both species can be considered to possess metal–metal double bonds. The metal–metal distances in $Nb_2Br_6(SC_4H_8)_3$ and $Ta_2Br_6(SC_4H_8)_3$ of 2.728 (5) and 2.710 (2) Å, respectively, compare favorably with d(Nb–Nb) = 2.70 Å reported for $Cs_3Nb_2Cl_9$[2] in spite of the larger size of the bridging sulfur and bromine atoms vs. chlorine. According to criteria for gauging metal–metal interactions in confacial bioctahedra proposed by Cotton and Ucko,[13] the bonding in the niobium and tantalum dimers reported here is similar to that found between molybdenum atoms in $Cs_3Mo_2Cl_9$[6] where d(Mo–Mo) = 2.66 Å and the formal bond order is 3. The difference between the Nb–Nb and Ta–Ta bond lengths determined here is hardly significant, and thus the great discrepancy in metal–metal bond lengths between $Mo_2X_9^{3-}$ [6] on one hand and $W_2Cl_9^{3-}$ [5] or $W_2Br_9^{2-}$ [15] on the other remains as an enigma.

Acknowledgment. We thank Professor Robert Jacobson for assistance with the structure determinations. This work was supported by the U.S. Department of Energy, Division of Basic Energy Sciences.

Registry No. $Nb_2Br_6(SC_4H_8)_3$, 38531-74-7; $Ta_2Br_6(SC_4H_8)_3$, 65651-12-9.

Supplementary Material Available: Listings of observed and calculated structure factors (20 pages). Ordering information is given on any current masthead page.

References and Notes

(1) To whom correspondence should be addressed.
(2) A. Broll, H. G. von Schnering, and H. Schäfer, *J. Less-Common Met.*, **22**, 243 (1970).
(3) E. T. Maas, Jr., and R. E. McCarley, *Inorg. Chem.*, **12**, 1096 (1973).
(4) J. L. Templeton and R. E. McCarley, to be submitted for publication.
(5) W. H. Watson and J. Waser, *Acta Crystallogr.*, **11**, 689 (1958).
(6) R. Saillant, R. B. Jackson, W. E. Streib, K. Folting, and R. A. D. Wentworth, *Inorg. Chem.*, **10**, 1453 (1971).
(7) (a) N. W. Alcock, presented in part at the International Summer School on Crystallographic Computing, Ottawa, Canada, Aug 1969; (b) J. D. Scott, Queen's University, Kingston, Ontario, Canada, personal communication, 1971.
(8) W. R. Busing, K. O. Martin, and H. A. Levy, "ORFLS, a Fortran Crystallographic Least Squares Program", Report ORNL-TM-305, Oak Ridge National Laboratory, Oak Ridge, Tenn., 1962.
(9) H. P. Hanson, F. Herman, J. D. Lea, and S. Skillman, *Acta Crystallogr.*, **17**, 1040 (1964).
(10) "International Tables for X-Ray Crystallography", Vol. III, Kynoch Press, Birmingham, England, 1962, pp 215–216.
(11) W. R. Busing, K. O. Martin, and H. A. Levy, "ORFEE, a Fortran Crystallographic Function and Error Program", Report ORNL-TM-306, Oak Ridge National Laboratory, Oak Ridge, Tenn., 1964.
(12) Supplementary material.
(13) F. A. Cotton and D. A. Ucko, *Inorg. Chim. Acta*, **6**, 161 (1972).
(14) R. Saillant and R. A. D. Wentworth, *J. Am. Chem. Soc.*, **91**, 2174 (1969).
(15) J. L. Templeton, R. A. Jacobson and R. E. McCarley, *Inorg. Chem.*, **17**, 3320 (1978).